

Multimode system condition monitoring using sparsity reconstruction for quality control

Wafa Bougheloum, Mounir Bekaik, Sofiane Gherbi

Laboratory of Automation and Signals Annaba, Department of Electronics, Faculty of Technology, Badji Mokhtar Annaba University, Annaba, Algeria

Article Info

Article history:

Received Apr 9, 2022

Revised Sep 27, 2022

Accepted Oct 1, 2022

Keywords:

Diagnosis

Process monitoring multivariate

statistical process control

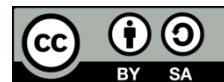
Stacked sparse autoencoder

data reconstruction

ABSTRACT

In this paper, we introduce an improved multivariate statistical monitoring method based on the stacked sparse autoencoder (SSAE). Our contribution focuses on the choice of the SSAE model based on neural networks to solve diagnostic problems of complex systems. In order to monitor the process performance, the squared prediction error (SPE) chart is linked with nonparametric adaptive confidence bounds which arise from the kernel density estimation to minimize erroneous alerts. Then, faults are localized using two methods: contribution plots and sensor validity index (SVI). The results are obtained from experiments and real data from a drinkable water processing plant, demonstrating how the applied technique is performed. The simulation results of the SSAE model show a better ability to detect and identify sensor failures.

This is an open access article under the [CC BY-SA](https://creativecommons.org/licenses/by-sa/4.0/) license.



Corresponding Author:

Wafa Bougheloum

Laboratory of Automation and Signals Annaba, Department of Electronics, Faculty of Technology, Badji Mokhtar Annaba University

Annaba, Algeria

Email: bougheloumwafa@gmail.com

1. INTRODUCTION

Industrial systems are becoming more and more complex, which makes it very difficult to control their various adjustment parameters. The difficulty comes not only from the fact that the control of an automated system requires real-time information on the various events, but also to detect failures and diagnose the reasons in order to find adequate solutions. The water industry is under increasing pressure to produce the highest quality drinking water at a lower cost. This implies a saving in terms of cost but also in terms of respect for the environment. The objective of this work is to present a model that allows the detection/diagnosis of the faults which can affect a station of treatment of drinking water based on data collected in real-time. Generally, the analytical methods used in the modeling of dynamic systems do not necessarily meet what is expected by automation engineers, hence the need to rely on statistical methods that provide more information on the processes from existing real data. In this sense, an approach for determining operational states based on data from the statistical analysis system (SAS) can play an important role in the detection and diagnosis of errors [1]. Thus, multivariate statistics tools have been the source of many techniques used in statistical process control (SPC). By the way, control charts are the ultimate tools for applying SPC. They make it possible to visualize the evolution of the process in order to identify the changes likely to modify its performance. On the other hand, the dimensions of the processes [2] and the collinearities that may exist between the variables, limit the effectiveness in terms of error isolation in the direct interpretation of these graphs. The advantage of this method is characterized by reducing the size of the variable space using projection methods which can reveal hidden information that can be better explained.

The most well-known statistical tool is principal component analysis (PCA) [3]. It provides robustness [4] in terms of extracting the relevant variation from the data, defining a set of principal components (PCs) consisting of a linear combination of the original variables. The scope of the PCA method is wide, from dimensional reduction to noise reduction and suppression, including data compression and defect detection. The major disadvantage of this method is that the PCs are general linear sets of all input variables. In addition, the coefficients of its sets are generally non-zero. Therefore, each principal component obtained may not have any practical significance. Sparse principal component analysis (SPCA) [5], [6] solves this problem and becomes one of the most widely used techniques for better interpretation of close-range structures by identifying spatial structures present in the data. In SPCA, the PCs that should be sparse are limited, which means, they have only a few non-zero entries in the original database. This has the advantage, among others, that the components are easier to interpret. Nevertheless, both PCA and SPCA are linear methods and cannot be handled effectively with non-linear variables. With data processing technology, deep neural networks [7] can effectively solve the problem of insufficient feature extraction methods [8].

In this work, we are interested in deep learning [9], which consists in learning high-level data representations using neural networks [10]. These methods were developed in the 1980s but were quickly abandoned because they were considered unpromising. With the improvement of computing power, new and richer databases [11], [12], and great advances in optimization techniques [13], [14], deep learning has recently reached exceptional performances for different tasks [15]–[17]. Then, we focus on the stacked sparse autoencoder (SSAE) [18], which finds a hidden representation in massive data by using a multi-layer encoder-decoder structure, where small abstract features are extracted to reconstruct the input data. Data reconstructed can be used to recover detected faulty data. In addition, it can be used to detect and isolate the faulty sensor through an analytical redundancy method that captures anomalies based on the divergence between the measurement data and the reconstructed one. Subsequently, after recovery, new feature detection is carried out by means of the Q-statistics [19] in combination with an adaptive nonparametric kernel density estimation (KDE) based limit of confidence in order to minimize the rate of faulty alert detection. Once the detection is performed, we need to know which sensor is faulty. To do this, we use one of the many defect identification methods that have been developed, such as contribution plots and sensor validity index (SVI).

In this work, the SSAE model is discussed, which is trained to reconstitute the collected input data in standard conditions. This article is structured through the following: section 2 outlines the process monitoring strategy based on spasticity reconstruction. In section 4, results are presented using both synthesized and real data collected from a potable water processing plant.

2. METHODS

2.1. Statistical process monitoring (SPM) method: stacked sparse autoencoder

Deep learning is a branch of machine learning. It consists of learning representations of the high level of data using neural networks. These methods have been developed in the 1980s but were quickly abandoned because considered not promising. Deep learning recently achieved exceptional performance for different tasks, however, in the area of process control, still rare. Deep neural network models are employed as a tool for predicting patterns that include a hidden layer called the bottleneck layer.

First, the input vector $x_i = \{1, 2, 3, \dots, N\}$ is transformed into a hidden part represented by the function h_i , which is as (1),

$$h_i = f(x_i) = \text{sigm}(W_1 x + b_1) \quad (1)$$

where W_1 and b_1 are respectively the weight and the bias between the input layer and the hidden part and $\text{sigm}(x)$ is a sigmoid function that is calculated as (2).

$$\text{sigm}(x) = (1 + \exp(-x))^{-1} \quad (2)$$

At the decode layer, h_i gets mapped to the output enunciated by \hat{x} . where we employ the activation function represented as (3),

$$\hat{x}_i = g(h) = \text{sigm}(W_2 h_i + b_2) \quad (3)$$

where W_2 and b_2 represent the weight and the bias from the hidden to the output layer, as well (\hat{x}). An autoencoder for which the learning parameter implies a sparsity penalty [20] is simply called SSAE [21] as shown in Figure 1.

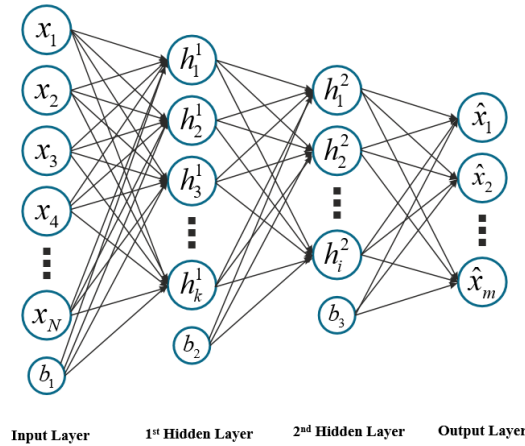


Figure 1. Structure of the proposed SSAE model

The power of this network consists in predicting its output (input estimate) to be as similar to its input, by optimizing the cost function given by (4),

$$J = \frac{1}{N} \sum_{i=1}^N \left(\frac{1}{2} \|\hat{x} - x_i\|^2 \right) + \frac{\lambda}{2} \sum_{i=1}^N \|W_i\|^2 + \beta \sum_{j=1}^m KL(\rho \|\hat{\rho}_j) \tag{4}$$

where m is the number of hidden nodes. λ and β are the coefficient determining the weight decay and the sparsity penalty terms respectfully. In (4), the first term is the reconstruction error, the second is the normalization term and the final one is the sparsity penalty, where $KL(\rho \|\hat{\rho}_i)$ is the Kullback-Leibler divergence, is used to compute the difference between ρ and $\hat{\rho}_i$ being the constraint used during learning. $KL(\rho \|\hat{\rho}_i)$ [22] is defined as (5).

$$KL(\rho \|\hat{\rho}_i) = \rho \log \frac{\rho}{\hat{\rho}_i} + (1 - \rho) \log \frac{1-\rho}{1-\hat{\rho}_j} \tag{5}$$

The goal in the use of the SSAE is to train it using the backpropagation algorithm and limited memory BFGS (L-BFGS) [23], to reduce the cost function, and to define the adequate parameters W_1, W_2, b_1, b_2 .

2.2. Novelty detection

There are few studies on fault detection processing to diagnose the root causes of malfunctions or to identify unexpected events in data sets, which differ from the norm. Among these studies are those based on residual analysis, which is based on a similarity test between measured and estimated data. The regular measure used is the squared prediction error (SPE) where:

$$Q = SPE = \sum_{i=1}^N (x_i - \hat{x}_i)^2 \tag{6}$$

N is the number of samples. In this paper, we propose an adaptive confidence limit by employing a k -means clustering algorithm in order to split the normal data of the full operating regime into smaller and possibly simpler local operating regimes.

2.2.1. Control limits

a. χ^2 Distribution (δ_α^2)

The control limit is the process variation that indicates when the process is out of control. The system is considered to be in its normal state of operation if $SPE \leq \delta_\alpha^2$. On the other hand, if $SPE > \delta_\alpha^2$, the system is considered faulty, where δ_α^2 denoted for the SPE control limit [24], that can be determined by a distribution of weighted x^2 ,

$$\delta = g\chi_{h,\alpha}^2 \quad g = \frac{v}{2m} \quad h = \frac{2m^2}{v} \tag{7}$$

with m and v being the estimated mean and variance of SPE, respectively.

- b. Threshold using k -means based on kernel density estimation (adaptive upper control limit KDE/AUCL_{KDE})

KDE is a robust tool for the nonparametric approximation of a probability density function for random variables at any given point in the support. However, with a sample matrix of n variables and m samples, the KDE of the density function $f(x)$ at each point x is written as:

$$f(x) = \frac{1}{mh} \sum_{j=1}^n K\left(\frac{x-x_j}{h}\right) \quad (8)$$

h is the border width setting and K is a kernel function that is integrable to one and has a null mean.

Many clustering algorithms for different problems have been proposed, including partition-based clustering, hierarchical clustering, neural network clustering, mixture model clustering, and kernel clustering. Many classification algorithms for various tasks have been developed such as fuzzy C-means [24]. The clustering algorithm that has been used in this paper is k -means. k -means is one of the simplest unsupervised learning algorithms that solve the well-known clustering problem. The procedure follows a simple and easy method to partition a data set via a number of classes (let us assume k classes) fixed a priori, where each partition represents a cluster containing at least one object. The objective of k -means is to minimize the objective function which is the total distance between all objects and their respective centers. These centers have to be placed in a clever way because a different location leads to a different result. The objective function is given as (9),

$$J = \sum_{j=1}^k \sum_{i=1}^n \|x_i^j - c_j\|^2 \quad (9)$$

where $\|x_i^j - c_j\|^2$ is a chosen distance measure between a data point x_i^j and the cluster center c_j , is an indicator of the distance of the n data points from their respective cluster centers. In the threshold-based clustering algorithm, we proceed as: an element is chosen from the dataset which is assigned as a seed of a cluster by the algorithm. Then we calculate the distance of each unclassified element from the cluster center. The element is assigned to the cluster if the distance is less than the threshold, otherwise, we recalculate the centers, if no cluster can be found after examining all elements in the cluster, then the element is assigned as a seed of a new cluster. If the distance between the new cluster and another cluster is less than the threshold, the two clusters are merged and the cluster distances are recalculated. After assigning all elements to a cluster, the algorithm stops.

3. FAULT IDENTIFICATION

3.1. Contribution plots

There are various approaches to fault isolation, for which contribution diagrams can be used. The contribution of variable j to the Q statistic is calculated as (10),

$$C_{ijk}^Q = e_{ijk}^2 \quad (10)$$

with $e = (x\hat{i} - x^{\wedge}i)$.

3.2. Nonlinear reconstruction principle

This approach is applied in the case of a faulty sensor. It consists of reconstructing the value measured by the sensor as a function of other variables in an iterative way as shown in Figure 2. The procedure consists in replacing the j^{th} variable with the predicted one and repeating it until the end of the algorithm as (11),

$$\tilde{x}_i = \xi_j^T G(F(x_j)) \quad (11)$$

with $\tilde{x}_i = (x_1, x_2, \dots, x^{\wedge}j, \dots, x_m)$, ξ^T is the j^{th} column of the identity matrix.

3.3. Sensor validity index

Its principle is to calculate the ratio between SPE _{j} and the faulty SPE, after calculating the SPE statistic of the same reconstructed variable [24], it is defined as (12),

$$\eta_j^2(k) = \frac{SPE_j(k)}{SPE(k)} \quad (12)$$

in which SPE is the overall squared prediction error obtained before the reconstruction and SPE j is the j th squared prediction error obtained after the reconstruction [25]. The validity index for a faulty sensor should tend to zero.

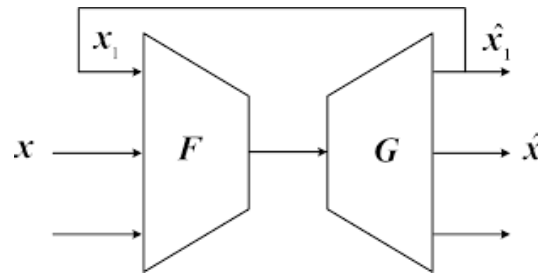


Figure 2. Reconstruction principle

4. RESULT AND DISCUSSION

4.1. Synthetic data

To illustrate the advantages of our developed method in fault detection and isolation, a multivariate dataset is used, containing three variables, where t is uniformly distributed in the interval $[-1, 1]$; ε_i represents Gaussian white noise with zero means and standard deviation of 0.01. 1,000 samples are collected to build SSAE model (13). After building the model, we examine the behavior of the SPE in normal conditions, where its threshold was calculated with three techniques: the χ^2 distribution, KDE, and the adaptive threshold AUCL_{KDE} using k -means clustering. The result is shown in Figure 3(a) SPE: data in normal state for δ^2 threshold, Figure 3(b) SPE: data in normal state for KDE threshold and Figure 3(c) SPE: data in normal state for AUCL threshold using k -means clustering. For simplicity of results, we use a window between 150 and 250 samples.

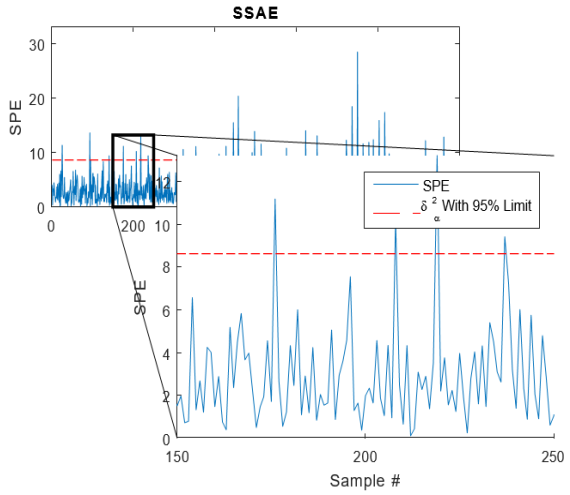
$$\begin{aligned} x_1 &= t^2 + 0.3 \sin(2\pi t) + \varepsilon_1 \\ x_2 &= t + \varepsilon_2 \\ x_3 &= t^3 + t + 1 + \varepsilon_3 \end{aligned} \quad (13)$$

We now simulate a bias fault and observe the variation of SPE with the three limits. Figure 4(a) to (c) show SPE data in the faulty state for δ^2 threshold, KDE threshold, and AUCL threshold using k -means clustering, respectively. By examining figures in normal and faulty modes, we observe false alarms in the data, generally from outliers. This model can detect the fault, there were 200 samples.

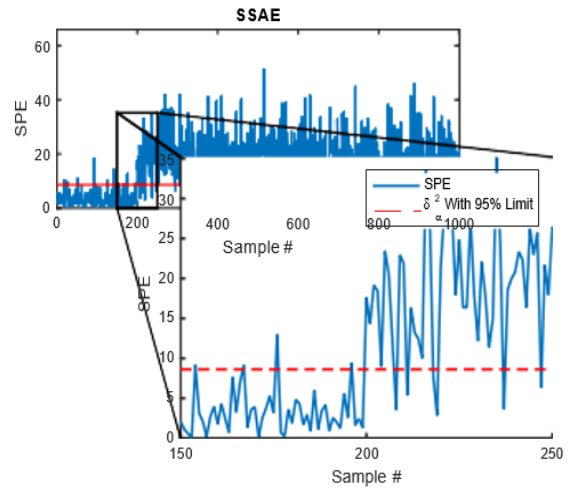
We have identified which sensor is faulty as shown in Figure 5(a) for SSAE model, the faulty one was the third. A second method of locating faulty sensors were used based on SVI. It returns the process to its normal operating conditions as shown in Figure 5(b).

4.2. Application on a water treatment plant

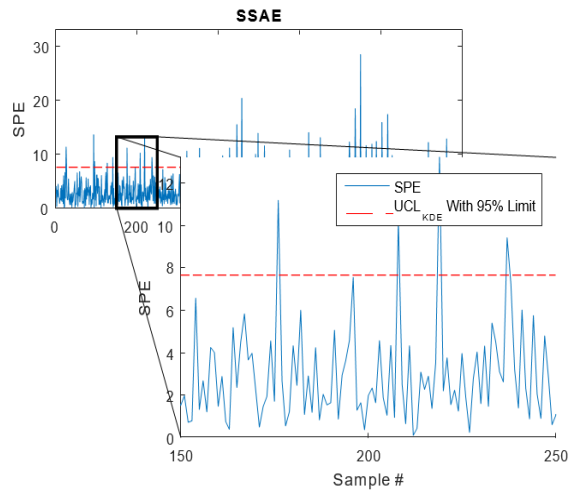
The factory that we studied is the purification of water in Oued El Othmania. It is responsible for the distribution of drinking water to many citizens at and around Constantine which is a city in northeast Algeria, it is also the third most populous city in the country [26]. It is known to have many important parameters such as turbidity, temperature, flow rate, and pH value. The data used in this study contains: raw water parameters and treated water parameters: turbidity, temperature, pH, and O₂, this means we have eight parameters in total, that is, we have eight sensors to be monitored. The observations are sampled by a data acquisition unit (SCADA system) for a period of 356 days, respecting various intervals. We use this database to construct and develop the model SSAE. The results are obtained from the PES under normal conditions with the three types of thresholds, which the real data are shown in Figure 6(a) to (c) for SPE data in the normal state for δ^2 threshold, KDE threshold, and AUCL threshold using k -means clustering, respectively. We add a defect to one of the sensors and we observe the result for the three thresholds as shown in Figure 7(a) to (c) for SPE data in the faulty state for δ^2 threshold, for the KDE threshold, and for AUCL threshold using k -means clustering, respectively. The SSAE model is able to detect the fault, in our example, the detection was made from sample 200. The faulty sensor was sensor 8 which is the treated water O₂ (TW) as demonstrated in Figure 8(a) for contribution plots and Figure 8(b) for SVI, which implies that the SSAE model is suitable for fault isolation.



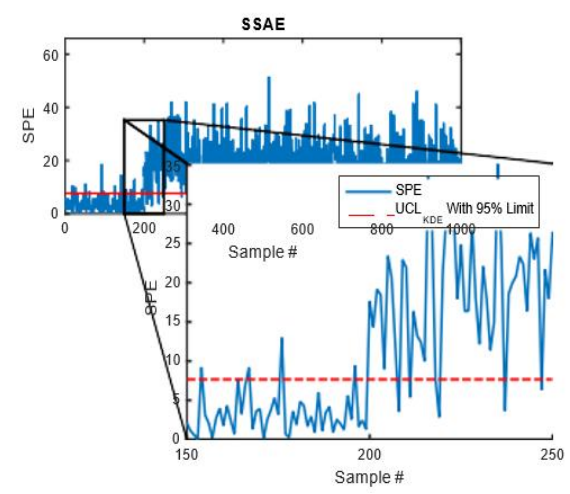
(a)



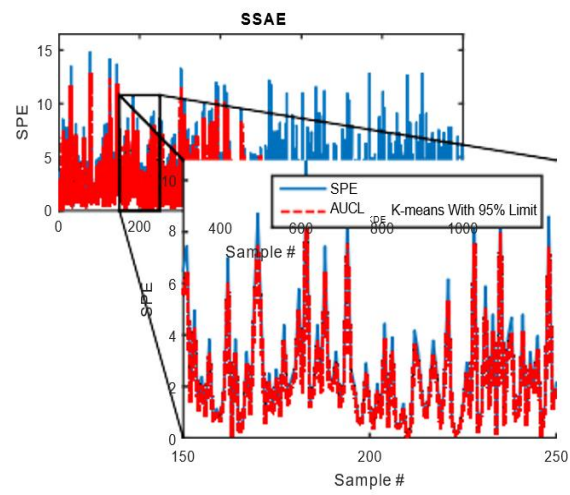
(a)



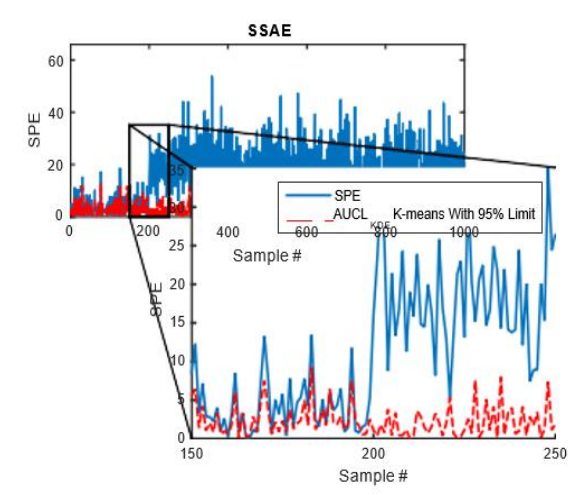
(b)



(b)



(c)



(c)

Figure 3. SPE data in normal state (a) δ_α^2 threshold, (b) KDE threshold, and (c) AUCL threshold using *k*-means clustering

Figure 4. SPE data in faulty state (a) δ_α^2 threshold, (b) KDE threshold, and (c) AUCL threshold using *k*-means clustering

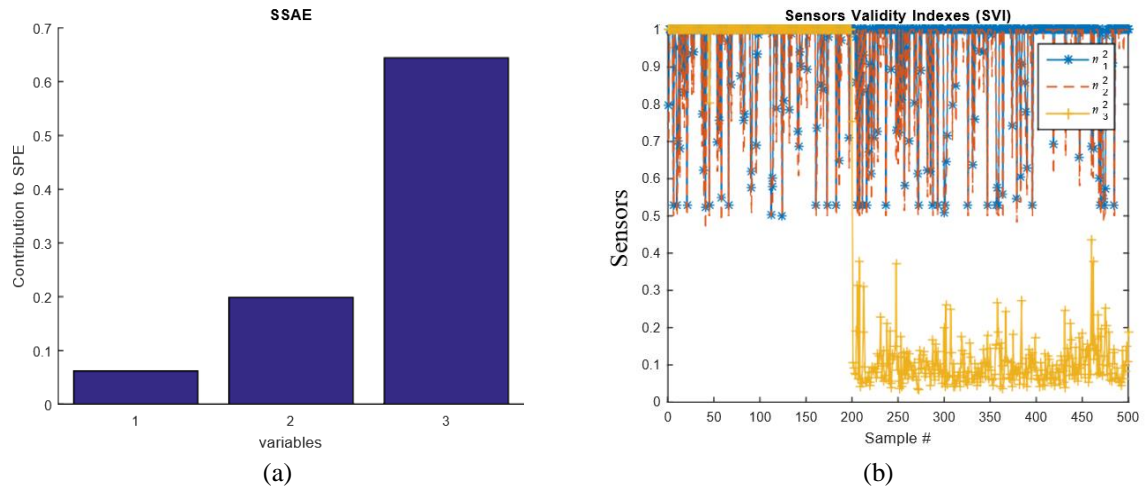


Figure 5. Fault isolation (a) normalized contribution plots (fault in the 3rd sensor) and (b) SVI sensor validity index (3rd sensor fault)

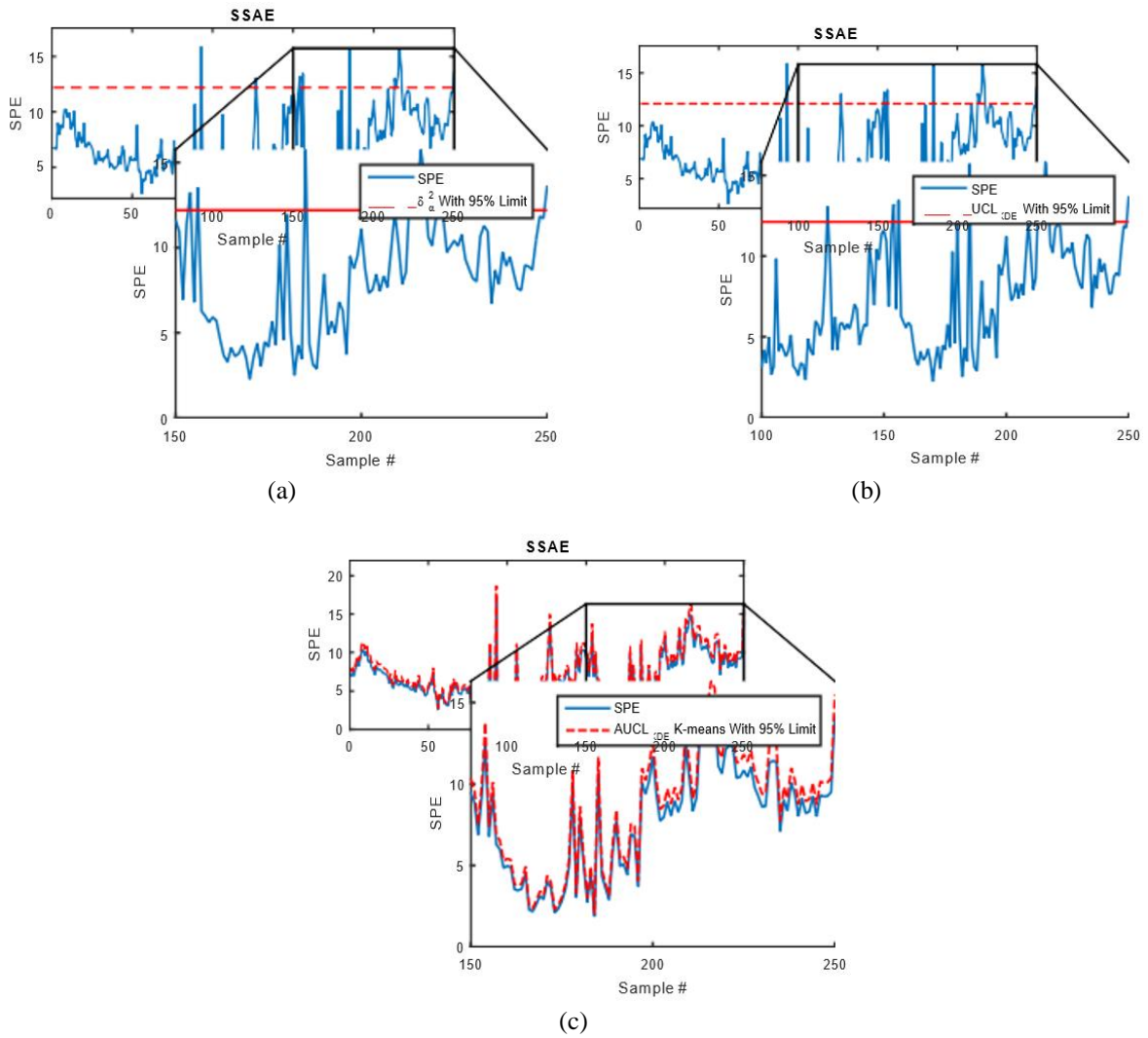


Figure 6. SPE data in normal state for (a) δ_α^2 threshold, (b) KDE threshold, and (c) AUCL using *k*-mean clustering

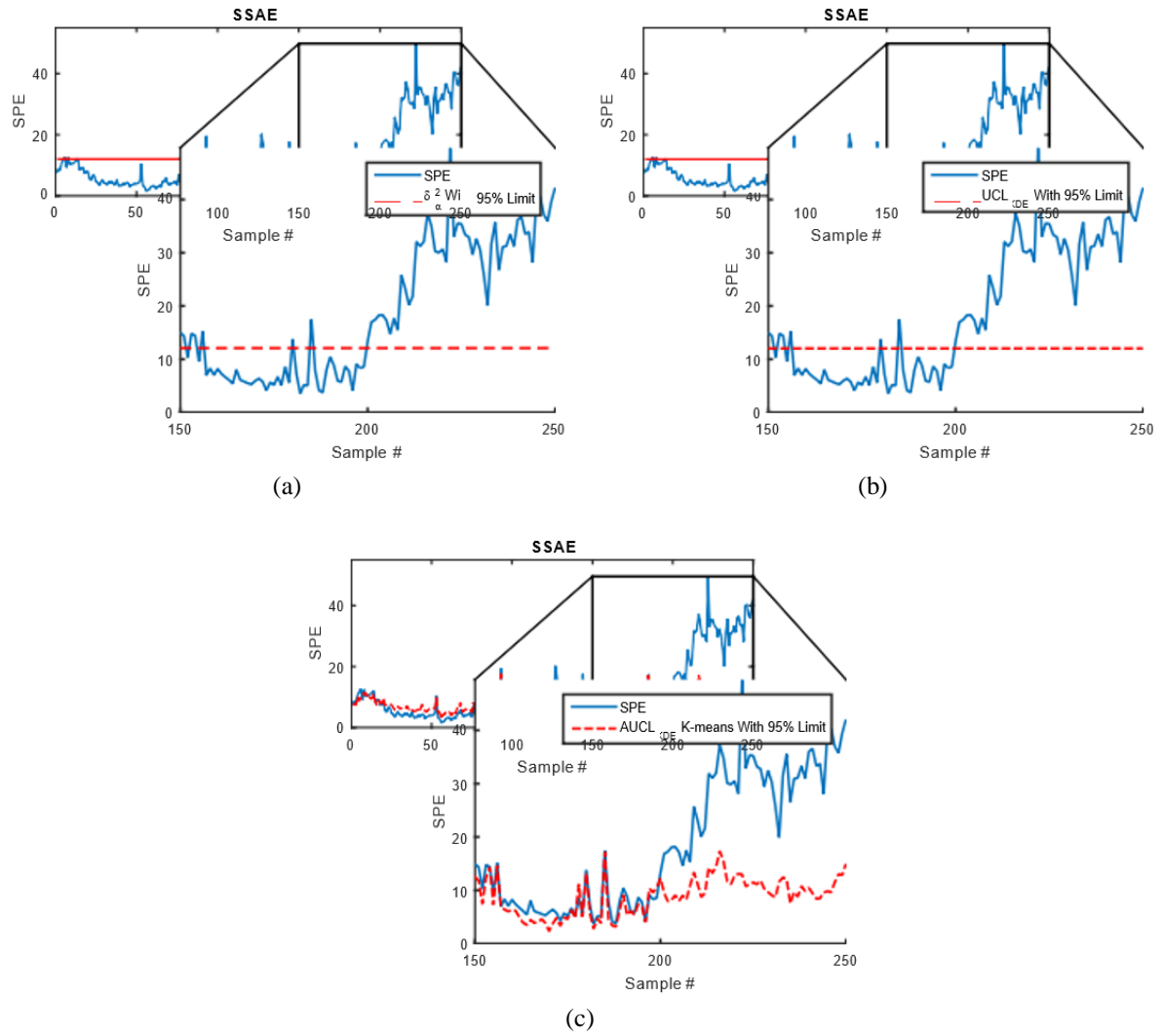


Figure 7. SPE data in faulty state for (a) δ_α^2 threshold, (b) KDE threshold, and (c) AUCL using k -mean clustering

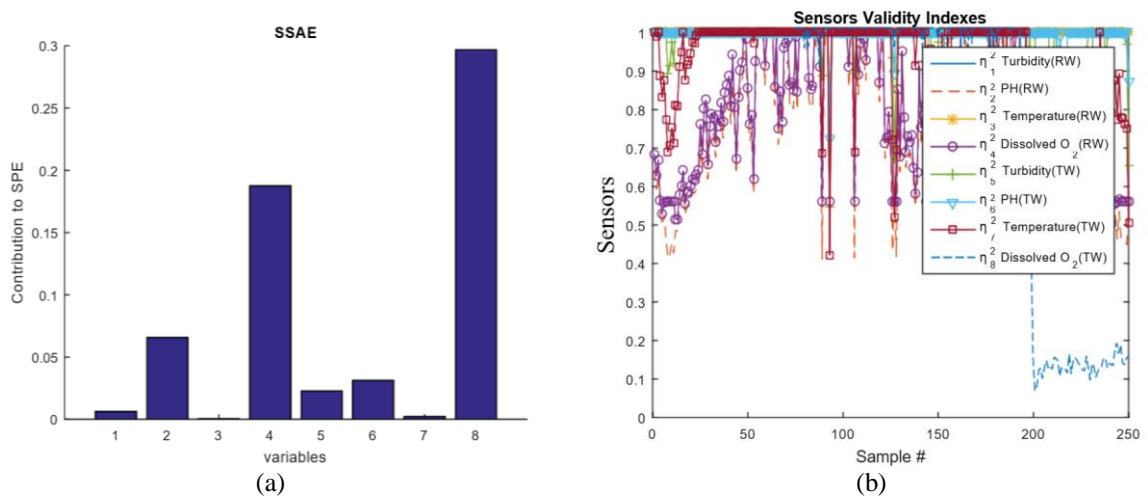


Figure 8. Fault isolation (a) normalized contribution plots (fault in the 8 sensor) and (b) SVI's raw water (RW) and treated water (TW) sensors

5. CONCLUSION

In this work, we propose an SSAE modeling method applied to real data collected from a drinking water treatment plant. We used the SPE index for the detection of the defects, by calculating its confidence limit by three different techniques: the χ^2 distribution, the KDE, and the upper control limit (UCL_{KDE}) with the k -means clustering, which allowed us to obtain a very good result. Then, we proceed to the localization of the faulty sensor using two approaches: Contribution diagrams and the improved SVI based on the reconstruction principle. Simulation results show that the choice of the SSAE model is effective in terms of the ability to detect and identify sensor failures. In terms of perspective and in order to reduce the overfitting problem and improve the performance of SSAE, we can adopt the dropout technique and rectified linear unit (ReLU) activation function to achieve high diagnostic accuracy.




REFERENCES

- [1] P. Datta, P. Das, and A. Kumar, "Hyper parameter tuning based gradient boosting algorithm for detection of diabetic retinopathy: an analytical review," *Bulletin of Electrical Engineering and Informatics (BEEI)*, vol. 11, no. 2, pp. 814–824, Apr. 2022, doi: 10.11591/eei.v11i2.3559.
- [2] A. Hussein Ali, R. A. I. Alhayali, M. A. Mohammed, and T. Sutikno, "An effective classification approach for big data with parallel generalized Hebbian algorithm," *Bulletin of Electrical Engineering and Informatics (BEEI)*, vol. 10, no. 6, pp. 3393–3402, Dec. 2021, doi: 10.11591/eei.v10i6.3135.
- [3] I. T. Jolliffe and J. E. Jackson, "A user's guide to principal components," *The Statistician*, vol. 42, no. 1, 1993, doi: 10.2307/2348121.
- [4] N. More, V. B. Nikam, and B. Banerjee, "Novel approach of association rule mining for tree canopy assessment," *IAES International Journal of Artificial Intelligence (IJ-AI)*, vol. 10, no. 3, pp. 771–779, Sep. 2021, doi: 10.11591/ijai.v10.i3.pp771-779.
- [5] I. T. Jolliffe and J. Cadima, "Principal component analysis: a review and recent developments," *Philosophical Transactions of the Royal Society A: Mathematical, Physical and Engineering Sciences*, vol. 374, no. 2065, Apr. 2016, doi: 10.1098/rsta.2015.0202.
- [6] H. Zou and L. Xue, "A selective overview of sparse principal component analysis," *Proceedings of the IEEE*, vol. 106, no. 8, pp. 1311–1320, Aug. 2018, doi: 10.1109/JPROC.2018.2846588.
- [7] P. Rajendran and K. Ganapathy, "Neural network based seizure detection system using statistical package analysis," *Bulletin of Electrical Engineering and Informatics (BEEI)*, vol. 11, no. 5, pp. 2547–2554, Oct. 2022, doi: 10.11591/eei.v11i5.3771.
- [8] M. C. G. Baabu and M. C. Padma, "Semantic feature extraction method for hyperspectral crop classification," *Indonesian Journal of Electrical Engineering and Computer Science (IJECS)*, vol. 23, no. 1, pp. 387–395, Jul. 2021, doi: 10.11591/ijeecs.v23.i1.pp387-395.
- [9] S. R. Salkuti, "A survey of big data and machine learning," *International Journal of Electrical and Computer Engineering (IJECE)*, vol. 10, no. 1, pp. 575–580, Feb. 2020, doi: 10.11591/ijece.v10i1.pp575-580.
- [10] S. Sharipuddin *et al.*, "Intrusion detection with deep learning on internet of things heterogeneous network," *IAES International Journal of Artificial Intelligence (IJ-AI)*, vol. 10, no. 3, pp. 735–742, Sep. 2021, doi: 10.11591/ijai.v10.i3.pp735-742.
- [11] H. Ohmaid, S. Eddarouich, A. Bourouhou, and M. Timouya, "Comparison between SVM and KNN classifiers for iris recognition using a new supervised neural approach in segmentation," *IAES International Journal of Artificial Intelligence (IJ-AI)*, vol. 9, no. 3, pp. 429–438, Sep. 2020, doi: 10.11591/ijai.v9.i3.pp429-438.
- [12] R. A. Hamzah, M. M. Roslan, A. F. bin Kadmin, S. F. bin A. Gani, and K. A. A. Aziz, "JPG, PNG and BMP image compression using discrete cosine transform," *Telecommunication Computing Electronics and Control (TELKOMNIKA)*, vol. 19, no. 3, Jun. 2021, doi: 10.12928/telkomnika.v19i3.14758.
- [13] Y. S. and N. Purnachand, "Convolutional neural network-based face recognition using non-subsampled shearlet transform and histogram of local feature descriptors," *IAES International Journal of Artificial Intelligence (IJ-AI)*, vol. 10, no. 4, pp. 1079–1090, Dec. 2021, doi: 10.11591/ijai.v10.i4.pp1079-1090.
- [14] A. Bustamam, M. I. Sunggawa, and T. Siswantining, "Performance of multivariate mutual information and autocorrelation encoding methods for the prediction of protein-protein interactions," *IAES International Journal of Artificial Intelligence (IJ-AI)*, vol. 11, no. 2, pp. 773–786, Jun. 2022, doi: 10.11591/ijai.v11.i2.pp773-786.
- [15] A. Dixit and T. Kasbe, "Multi-feature based automatic facial expression recognition using deep convolutional neural network," *Indonesian Journal of Electrical Engineering and Computer Science (IJECS)*, vol. 25, no. 3, pp. 1406–1419, Mar. 2022, doi: 10.11591/ijeecs.v25.i3.pp1406-1419.
- [16] Y. S. and P. N., "An effective face recognition method using guided image filter and convolutional neural network," *Indonesian Journal of Electrical Engineering and Computer Science (IJECS)*, vol. 23, no. 3, pp. 1699–1707, Sep. 2021, doi: 10.11591/ijeecs.v23.i3.pp1699-1707.
- [17] S. A. Shawkat and I. Al-Barazanchi, "A proposed model for text and image encryption using different techniques," *Telecommunication Computing Electronics and Control (TELKOMNIKA)*, vol. 20, no. 4, Aug. 2022, doi: 10.12928/telkomnika.v20i4.23367.
- [18] J. Xu *et al.*, "Stacked sparse autoencoder (SSAE) for Nuclei detection on breast cancer histopathology images," *IEEE Transactions on Medical Imaging*, vol. 35, no. 1, pp. 119–130, Jan. 2016, doi: 10.1109/TMI.2015.2458702.
- [19] D. A. White *et al.*, "Low open-area endpoint detection using a PCA-based T/sup 2/ statistic and Q statistic on optical emission spectroscopy measurements," *IEEE Transactions on Semiconductor Manufacturing*, vol. 13, no. 2, pp. 193–207, May 2000, doi: 10.1109/66.843635.
- [20] H. Larochelle, Y. Bengio, J. Louradour, and P. Lamblin, "Exploring strategies for training deep neural networks," *Journal of machine learning research*, vol. 10, no. 1, 2009.
- [21] J. Ou, H. Li, G. Huang, and Q. Zhou, "A novel order analysis and stacked sparse auto-encoder feature learning method for milling tool wear condition monitoring," *Sensors*, vol. 20, no. 10, May 2020, doi: 10.3390/s20102878.
- [22] P. Vincent, H. Larochelle, I. Lajoie, Y. Bengio, P.-A. Manzagol, and L. Bottou, "Stacked denoising autoencoders: Learning useful representations in a deep network with a local denoising criterion," *Journal of machine learning research*, vol. 11, no. 12, 2010.
- [23] D. C. Liu and J. Nocedal, "On the limited memory BFGS method for large scale optimization," *Mathematical Programming*, vol. 45, no. 1–3, pp. 503–528, Aug. 1989, doi: 10.1007/BF01589116.




- [24] W. Bougheloum and M. Ramdani, "Accurate quality control charts via sparsity reconstruction for multimode process monitoring," *International Journal of Control, Energy and Electrical Engineering (CEEE)*, vol. 11, pp. 8–11, 2019.
- [25] K. Bouzenad, M. Ramdani, N. Zermi, and K. Mendaci, "Use of NLPCA for sensors fault detection and localization applied at WTP," in *2013 World Congress on Computer and Information Technology (WCCIT)*, Jun. 2013, pp. 1–6, doi: 10.1109/WCCIT.2013.6618761.
- [26] K. Mendaci, M. Ramdani, and T. Benzaraa, "Nonlinear multivariate statistical process monitoring of a water treatment plant," in *2013 5th International Conference on Modeling, Simulation and Applied Optimization (ICMSAO)*, Apr. 2013, pp. 1–6, doi: 10.1109/ICMSAO.2013.6552651.

BIOGRAPHIES OF AUTHORS






Wafa Bougheloum    received her M.Sc. degree in Automation Control from Annaba University in 2012. She is currently pursuing a Ph.D. degree in automation control at Badji Mokhtar Annaba University Algeria. Her research interests include fault diagnosis, multivariate statistical approaches, process modeling, and monitoring. She can be contacted at email: bougheloumwafa@gmail.com.



Mounir Bekaik    is a lecturer of Automation Control at Annaba University Algeria. He received his M.Sc. degree in Automation Control from Supelec, Paris, France in 2010 and his Ph.D. degree in automation control from Supelec, Paris, France in 2013. His research interests include control of nonlinear systems, robustness, and intelligent control. He can be contacted at email: Mounir.bekaik@univ-annaba.dz.



Sofiane Gherbi    is a full professor of automatic control systems at Annaba University, Algeria. He received his Ph.D. degree in automatic control systems from the same university in 2009. His research interests include robust control, delay systems, networked control system, and intelligent control. He can be contacted at email: sofiane.gherbi@univ-annaba.dz.